Evaluation of Tracking Algorithms for Automated Strain Analysis on Fascial Tissue

Mirko Halbe, Oliver Wetter,
Torben Wallenstein, and Jan-Philipp Schulze
Hochschule Bielefeld
University of Applied Sciences and Arts
Minden, Germany

Jörg Höer
Hochtaunus Kliniken
Department for General and Visceral Surgery
Bad Homburg, Germany

***Abstract*—The development of detailed fascial tissue models is an essential aspect in research of medical suture failure. These models can be created on the basis of tensile test data and require accurate deformation measurement. Typically, this is done by applying colored dots or a speckle pattern to simplify the tracking with digital image correlation (DIC). This method leads to time-consuming preparation of the test objects and a computationally intensive analysis. This paper presents an alternative approach to automated strain analysis, using open-source tracking algorithms to measure the deformation of natural textures on fascial tissue. As part of the evaluation, a strain-dependent error in the displacement of individual tracking points was identified using artificial videos of idealized stretched fascial textures. By automating and simplifying the deformation measurement, the described approach enables researchers to easily investigate various different fascial tissue samples in order to generate more characteristic data and improve existing models.**

***Index Terms*—Tensile test, fascial tissue analysis, texture tracking, OpenCV**

I. Introduction

Medical suture failure is a common complication following surgical closure of the abdominal wall and the surgical complication that most frequently leads to re-operation [1]. Concepts for avoiding these complications have long been part of research in biomechanics. A possible approach is to model the elastic behavior of fascial tissue in order to understand its mechanical properties and enable finite element method (FEM) simulations. This approach has been the subject of numerous medical and biomechanical publications [2] [3] [4]. These models require measurements of local stress and strain conditions as characteristic material properties, which are typically determined by tensile tests with a video extensometer. There are various approaches in the literature for analyzing video material of an inhomogeneous test specimen during a tensile test. For example, Cooney et al. uses a static number of reference points applied to the test specimens [3] [4] and Elliott et al. uses colored reference lines on the test specimens that are analyzed by Harris Corner Detection to determine the displacement [5]. Another common approach used by Jacquemoud et al. and Chen et al. is to apply a random speckle pattern to the test specimens and then use DIC to analyze the displacement [6] [7]. Santamaria et al. extended this method by using two cameras in a stereo DIC, which was also used by Kroese et al. and Estermann et al. [2] [8] [9]. These methods all have in common that the test specimens must be colored prior to the tensile test. Although previous studies have shown that a thin layer of color has a negligible influence on the mechanical properties [10], it is desirable to simplify the preparation process of the test specimens. This aspect becomes even more important for analyzing a large number of samples to improve the statistical significance of the fascia model. Cheng et al. developed a DIC modification for natural textures that does not require speckle patterns, but has the disadvantage of increased computational demands [11]. This paper presents and evaluates an alternative approach to automated strain analysis of fascial tissue, using natural textures and common open-source tracking algorithms. Therefore different tracking algorithms provided by the open-source computer vision library OpenCV are introduced and evaluated regarding their tracking performance.

II. Experimental Setup and Preprocessing

The experimental setup is designed to perform uniaxial tests using the universal testing machine 'Hegewald & Peschke inspekt table 10 kN'. For this purpose, the used porcine test specimens are fixed with two clamping jaws at the lower and upper mounting points of the machine, as shown in Fig. 1.

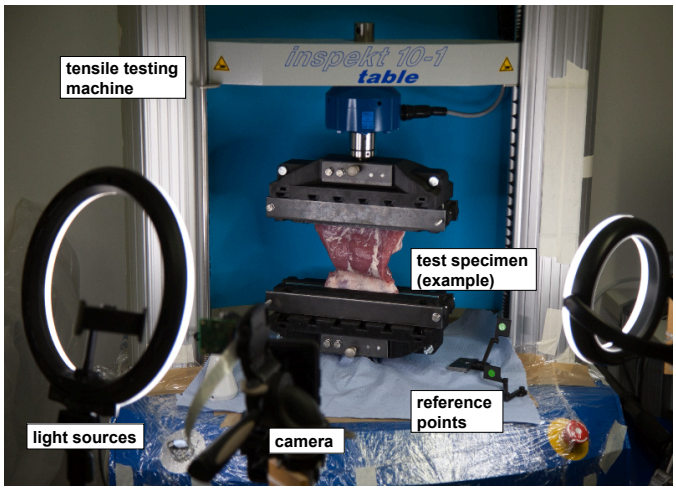

Fig. 1: Experimental setup with tensile testing machine, camera position, light sources and a test specimen

Light sources are used to ensure constant ambient lighting for video analysis, and reference points with known diameters are used to scale the measured data from pixels to millimeters. The simple smartphone camera of a Samsung SM-A528B with a video resolution of 2160 x 3840 pixels and a frame rate of 30 frames per second is used to record the videos. The automated deformation video analysis requires a preprocessing procedure for every frame. The part of the image showing the test specimen gets isolated by applying a color mask and then performing binary encoding. Assuming an approximately quadrangular object, the corner points can be determined by applying the Douglas-Peuker algorithm on the contours of the binary image [12]. The algorithm approximates the contour with less vertexes of a given precision that can be adjusted by a parameter γ. With a suitable value for γ, the corner points of the largest detected quadrangular object achieve an acceptable approximation to the corner points of the test specimen. For the first frame, the initial texture regions for tracking (tracking rectangles) can then be placed equidistant between the lower and the upper edge of the object. Depending on the particular application, a different arrangement of tracking rectangles can also be selected. The preprocessing steps are shown in Fig. 2.

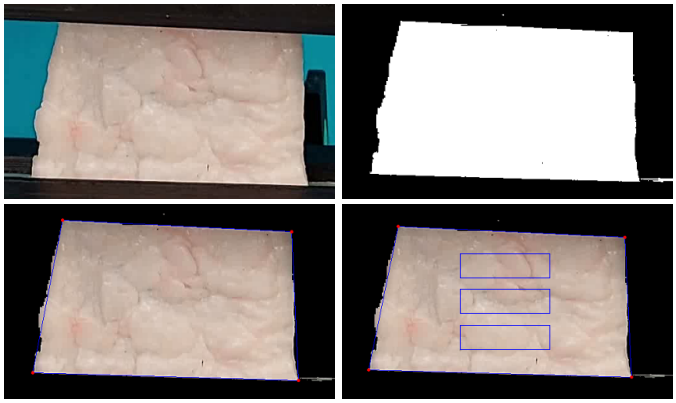

Fig. 2: Preprocessing steps: Initial frame, color mask and binary image, corner detection, and initial tracking rectangles

The idea of using tracking algorithms is to continuously update rectangular regions by successively monitoring the fascial texture within each region for every video frame. By treating each fascial texture as a trackable object, standard object tracking algorithms can determine the spatial displacement of these regions.

III. Validation of Common Tracking Algorithms with Synthetic Data

Typical algorithms for this use case are provided by the OpenCV tracking API, which enables easy application and comparison of different algorithms [13]. This paper validates seven tracking algorithms provided by the OpenCV tracking API in version 4.5.0. These are *discriminative correlation filter with channel and spatial reliability* (CSRT) [14], *generic object tracking using regression network* (GOTURN) [15], *kernelized correlation filter* (KCF) [16], *median flow algorithm* (MF) [17], *multiple instance learning* (MIL) [18], *minimum output sum of squared error* (MOSSE) [19], and *tracking, learning, detection* (TLD) [20]. For a general benchmark of these algorithms, reference is made to Dardagan et al. [21]. The following analysis applies the algorithms to measure the displacement of predefined tracking rectangles on natural fascial tissue textures for multiple test specimens.

A validation of the applicability of these tracking algorithms on fascial tissue textures in a real tensile test is challenging. As the displacement of the tissue is inhomogeneous, no ground truth can be defined. For this reason, synthetic data are generated from a simulation of the tensile test. The experimental setup is modeled using the graphics software 'Blender' [22] with light sources and the camera position according to the original experiment. In the simulation, images of real test specimens are displaced and elongated linearly and homogeneously in order to generate synthetic data of the tensile test. Due to the known displacement, the ground truth can be determined and compared to the results of the algorithms. The horizontal and vertical deformation velocity is chosen similarly to the original experiment. The simulation setup can be seen in Fig. 3.

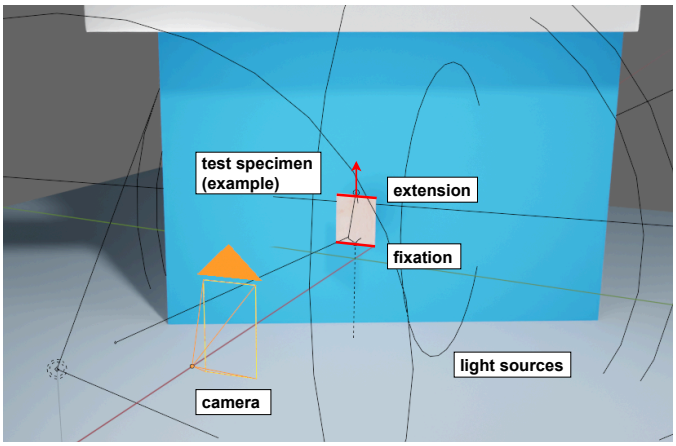

Fig. 3: Simulation setup for generating synthetic data

The validation aims to identify suitable algorithms for texture tracking on fascial tissue. Therefore, one tracking rectangle is defined in the center of the simulated test specimen for each algorithm. The test specimen is elongated to double the initial length, and the tracking accuracy can be determined by comparing the results of the algorithms with the calculated ground truth. Within the scope of the validation, seven different images of fascial tissue patterns are used. It can be observed that the TLD algorithm is subject to large jumps of the tracked area and the GOTURN algorithm fails completely for various test specimens. These algorithms are consequently unsuitable for tracking fascial tissue textures. Fig. 4 shows an exemplary test series for comparing the performance of the algorithms. It can be seen that the CSRT algorithm achieves good qualitative performance in this test while the tracking with KCF, MedianFlow, MIL and MOSSE is comparatively inaccurate. A high accuracy of the CSRT algorithm at lower

speed compared to other tracking methods was also confirmed in a benchmark with other video data by Dardagan et al. [21].

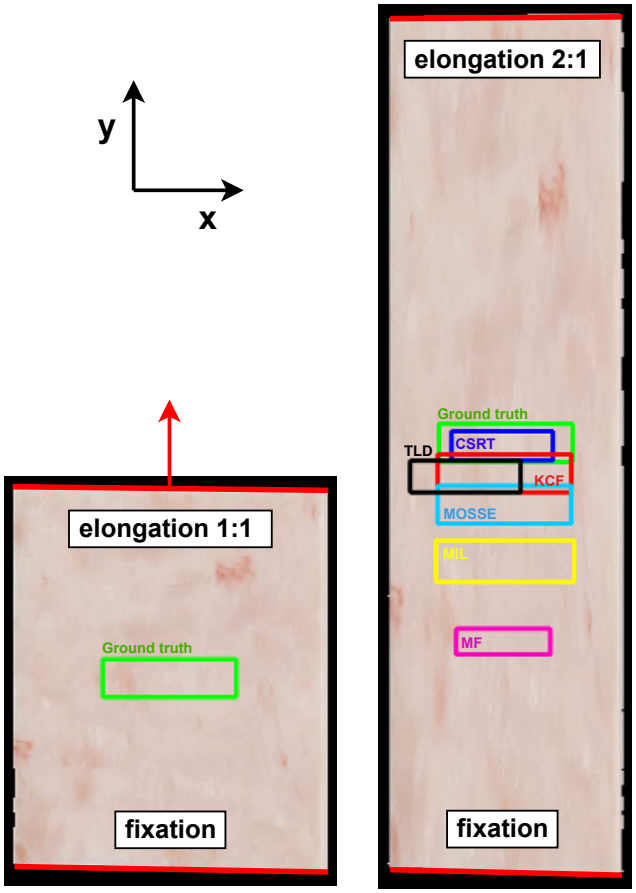

(a) Initial frame (b) Final frame

Fig. 4: Comparison of Ground truth (green) and the tracking algorithms CSRT (blue), KCF (red), MF (magenta), MIL (yellow), MOSSE (cyan), TLD (black) with synthetic data

IV. Verification of CSRT tracking algorithm

Based on these results, the accuracy of the CSRT tracking algorithm for fascial texture is examined in detail. Two different studies are carried out: In a first test series, the image of a fascial texture is linearly displaced without any stretching. In a second test series, the image is homogeneously elongated similar to the validation and the real tensile test. As part of the investigation, 49 displacement tests and 56 elongation tests were carried out. The maximum considered strain is 0.7, because higher strains usually lead to tearing of real test samples. The height of the test specimen in the simulation is about 300 pixels and thus chosen similar to the height in the real experiment. In the case of linear translation, the amount of displacement can be used directly as ground truth for all tracking rectangles. For the homogeneously elongated fascial texture, the ground truth can be calculated from the initial placement and the displacement of the upper edge. The calculated error is considered in vertical direction, as this is the significant variable in the context of a real tensile test. In Fig. 5 the position error of the tracking rectangles is shown with a color scheme according to the distribution of the deviation that can be found in Fig. 6. A trace is displayed in orange if at least one sample is outside the 2σ interval, or in red if at least one sample is outside the 3σ interval.

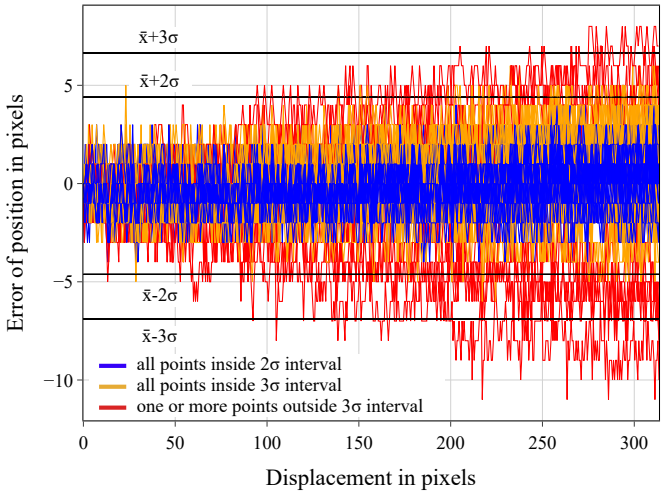

Fig. 5: Position error of the displacement tests

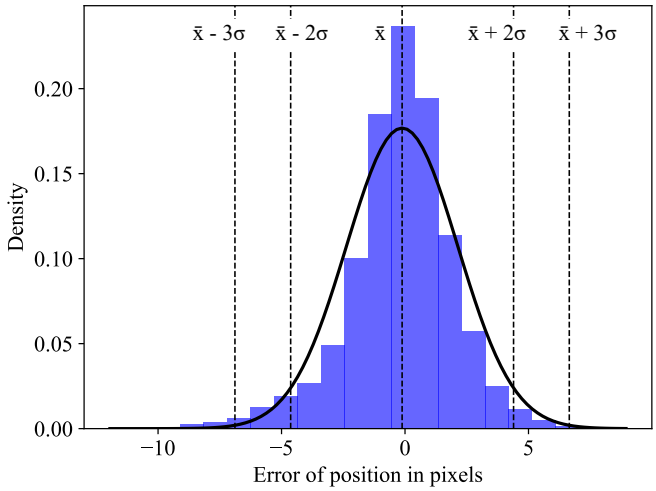

Fig. 6: Histogram of the displacement test

Fig. 6 shows that the position error of the displacement test is approximately normally distributed. Also, a proportional relationship between the position error and the displacement in pixels can be inferred from Fig. 5. For the second test using homogeneously elongated test specimens, the position error of the tracking rectangles is shown as a function of the strain in Fig. 7. The corresponding distribution can be found in Fig. 8. As in the first experiment, the color scheme is determined according to the σ-intervals. Also for the elongation test, an approximately normally distributed error can be found in Fig. 8 and a proportional relationship between position error and strain can be inferred from Fig. 7.

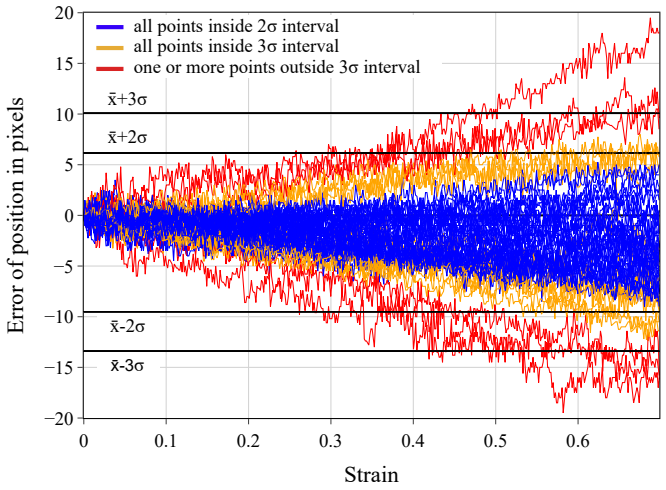

Fig. 7: Position error of the elongation test

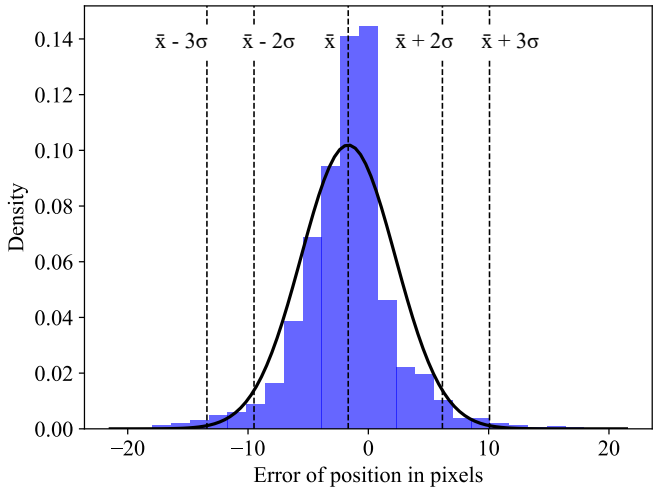

Fig. 8: Histogram of the elongation test

A comparison of Fig. 5 and Fig. 7 reveals that the measured position errors of the elongation tests are generally higher compared to the displacement tests. This is because the texture within the tracking rectangle changes during the elongation tests, making precise tracking more difficult. The position error of the displacement tests is linearly dependent on the displacement, which can be seen in Fig. 5. The calculated mean position error is $\bar{x}_d = -0.12$ pixels and the standard deviation is $\sigma_d = 2.26$ pixels. The position error of the elongation tests is linearly dependent on the strain itself, which can be seen in Fig. 7. This results from the idealized, homogeneous strain ϵ, which has the same effect on every defined tracking rectangle. Assuming that texture deformation within the tracking rectangles causes the position error, the same position error can be expected for all tracking rectangles. The calculated mean position error is $\bar{x}_e = -1.67$ pixels and the standard deviation is $\sigma_e = 3.91$ pixels.

Looking at the data raises the question of whether there is a reason for the higher error values of some tracking rectangles. After a detailed inspection of the red synthetic data in Fig. 5 and Fig. 7, a relatively low contrast of the fascial texture inside the initial tracking rectangle can be found. The standard deviation of the gray-scaled initial tracking rectangle as a metric of contrast over the position error in pixels is shown in Fig. 9. The previously identified outliers with values outside the 3σ interval are marked as red dots. It is evident that low contrast indicates a high position error, which makes it difficult to track the textures. This results in the possibility of preselecting the initial tracking rectangles based on contrast values to reduce the error of the tracking method.

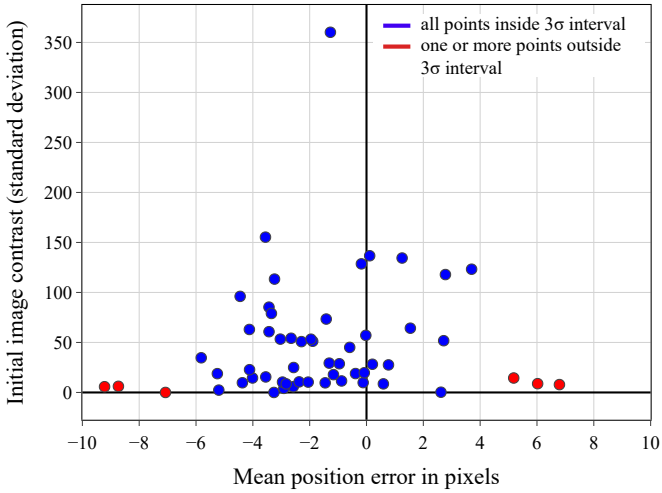

Fig. 9: Dependency between contrast of the image and the mean position error

V. Application to a real tensile test

After verification of the CSRT tracking algorithm and determination of the error, the tracking method is applied exemplarily to a real tensile test experiment. Therefore, three tracking rectangles are placed on the test specimens, as described in section II. During the data analysis two challenges arise in particular: The distance of two tracking rectangles can only be determined in discrete pixels, whereas the real object extends continuously. In addition, the tracking algorithms occasionally misidentify small single frame jumps of the fascial texture, leading to measurement outliers. The data quality can be significantly improved by applying a median filter to remove outliers and a gaussian filter to smooth the data and remove the influence of discrete pixel levels. Both filters are first preloaded with the first available value, which results in a stronger weighting of the first values. Fig. 10 presents the raw data and filtered data for a measured distance between two tracking rectangles from a real tensile test, plotted over the strain. It can be seen that the chosen filter method works well on this example.

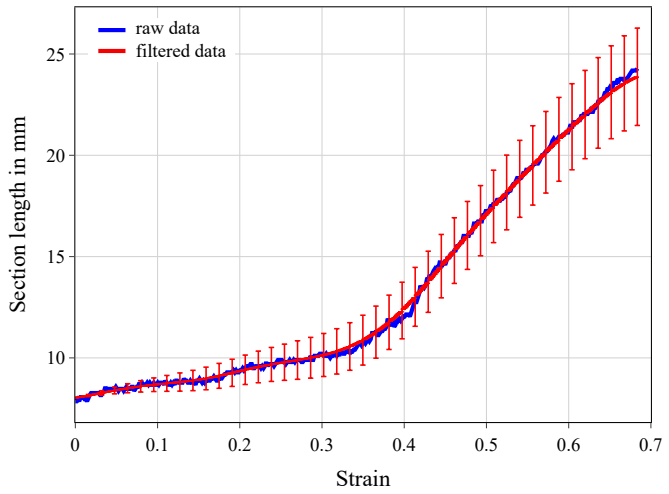

Fig. 10: Raw data (blue) and filtered data (red) of a section length measurement

Based on the described strain-dependent position error, the resulting error of a measured length L between two tracking rectangles can be calculated as

$$\frac{\Delta L}{L}(\epsilon) = 2 \cdot m \cdot \frac{\epsilon}{\epsilon_{max}} \tag{1}$$

The factor 2 is used to consider the position error of both the upper and lower tracking rectangles, and the factor $m = 3\sigma_e$ reflects the 3σ interval, which was determined with the elongation tests. The overall strain ϵ is used as an approximation for the local strain of each tracking rectangle with ϵ_{max} as the maximum strain taken into account in the elongation tests. The resulting error pipes are shown in Fig. 10. Since the position error of each tracking rectangle is given in pixels, it can be concluded that a higher video resolution leads to more accurate measurement results.

VI. Conclusion and Future Work

In this paper, a novel approach using tracking algorithms for an automated strain analysis on fascial tissue was presented. Compared to established methods, the advantages are rapid preparation and fast automated video analysis. Current limitations of the proposed method include the need for approximately rectangular test specimens and the examination of linear elongation, whereas real test specimens elongate nonlinearly. The developed preprocessing procedure was introduced and different open-source algorithms were compared in respect of their ability to track a predefined texture on a test specimen. A synthetic video data set was used for this purpose, enabling the definition of a ground truth for evaluating the tracking performance. In this experiment, the CSRT algorithm achieved the best overall results and was consequently evaluated in more detail by performing displacement and elongation tests with the synthetic video data. In these experiments, the position error of the tracked textures was characterized and found to be proportional to the strain of the test specimens. Based on these results, the presented approach can be applied to analyze the data of real tensile tests and characterize the position error.

In future work, more tracking algorithms should be investigated regarding their performance to track fascial tissue textures. More recent tracking algorithms based on deep learning are particularly interesting, as they could outperform the CSRT algorithm in terms of robustness and speed. As an extension of the validation process, the CSRT algorithm can be applied to a synthetic data set with nonlinear elongation and to a larger set of real test data. In addition, the applicability for real-time video analysis, the influence of different sizes and shapes of the tracked textures, and the investigation of the algorithms computational demands are interesting areas of research. Finally, the presented approach extends beyond the analysis of fascial tissue and can be generalized to track the deformation of other materials with a distinct surface texture.

References

[1] L. Xing, E. J. Culbertson, Y. Wen, and M. G. Franz, "Early laparotomy wound failure as the mechanism for incisional hernia formation," *Journal of Surgical Research*, vol. 182, no. 1, pp. e35–e42, 2013, doi: 10.1016/j.jss.2012.09.009.

[2] V. Acosta Santamaría, O. Siret, P. Badel, G. Guerin, V. Novacek, F. Turquier, and S. Avril, "Material model calibration from planar tension tests on porcine linea alba," *Journal of the Mechanical Behavior of Biomedical Materials*, vol. 43, pp. 26–34, 2015, doi: 10.1016/j.jmbbm.2014.12.003.

[3] G. M. Cooney, K. M. Moerman, M. Takaza, C. Des Winter, and C. K. Simms, "Uniaxial and biaxial mechanical properties of porcine linea alba," *Journal of the Mechanical Behavior of Biomedical Materials*, vol. 41, pp. 68–82, 2015, doi: 10.1016/j.jmbbm.2014.09.026.

[4] G. M. Cooney, S. P. Lake, D. M. Thompson, R. M. Castile, C. Des Winter, and C. K. Simms, "Uniaxial and biaxial tensile stress-stretch response of human linea alba," *Journal of the Mechanical Behavior of Biomedical Materials*, vol. 63, pp. 134–140, 2016, doi: 10.1016/j.jmbbm.2016.06.015.

[5] J. Elliott, S. Khandare, A. A. Butt, M. Smallcomb, M. E. Vidt, and J. C. Simon, "Automated tissue strain calculations using harris corner detection," *Annals of Biomedical Engineering*, vol. 50, no. 5, pp. 564–574, 2022, doi: 10.1007/s10439-022-02946-9.

[6] C. Jacquemoud, K. Bruyere-Garnier, and M. Coret, "Methodology to determine failure characteristics of planar soft tissues using a dynamic tensile test," *Journal of Biomechanics*, vol. 40, no. 2, pp. 468–475, 2007, doi: 10.1016/j.jbiomech.2005.12.010.

[7] T. Y.-F. Chen, N. M. Dang, Z.-Y. Wang, L.-W. Chang, W.-Y. Ku, Y.-L. Lo, and M.-T. Lin, "Use of digital image correlation method to measure bio-tissue deformation," *Coatings*, vol. 11, no. 8, p. 924, 2021, doi: 10.3390/coatings11080924.

[8] L. F. Kroese, J. J. Harlaar, C. Ordrenneau, J. Verhelst, G. Guérin, F. Turquier, R. H. M. Goossens, G.-J. Kleinrensink, J. Jeekel, and J. F. Lange, "The 'abdoman': An artificial abdominal wall simulator for biomechanical studies on laparotomy closure techniques," *Hernia*, vol. 21, no. 5, pp. 783–791, 2017, doi: 10.1007/s10029-017-1615-x.

[9] S.-J. Estermann, D. H. Pahr, and A. Reisinger, "Hyperelastic and viscoelastic characterization of hepatic tissue under uniaxial tension in time and frequency domain," *Journal of the Mechanical Behavior of Biomedical Materials*, vol. 112, p. 104038, 2020, doi: 10.1016/j.jmbbm.2020.104038.

[10] D. Zhang, C. D. Eggleton, and D. D. Arola, "Evaluating the mechanical behavior of arterial tissue using digital image correlation," *Experimental Mechanics*, vol. 42, pp. 409 – 416, 2002, doi: 10.1177/001448502321548247.

[11] X. Cheng, S. Wang, H. Wei, L. Li, Z. Huo, C. Li, and Z. Wang, "Digital image correlation by natural textures on biological skin," *Optics and Lasers in Engineering*, vol. 165, p. 107547, 2023, doi: 10.1016/j.optlaseng.2023.107547.

[12] D. H. Douglas and T. K. Peucker, “Algorithms for the reduction of the number of points required to represent a digitized line or its caricature,” *Cartographica*, vol. 2, pp. 112–122, 1973, doi: 10.3138/FM57-6770-U75U-7727.

[13] OpenCV. (2025) tracker.hpp file reference. [Online]. Available: https://docs.opencv.org/4.5.0/df/ddd/tracker_8hpp.html

[14] A. Lukezic, T. Vojir, L. C. Zajc, J. Matas, and M. Kristan, “Discriminative correlation filter with channel and spatial reliability,” *2017 IEEE Conference on Computer Vision and Pattern Recognition (CVPR)*, pp. 4847–4856, 2017, doi: 10.1109/CVPR.2017.515.

[15] D. Bolme, J. R. Beveridge, B. A. Draper, and Y. M. Lui, “Visual object tracking using adaptive correlation filters,” in *2010 IEEE Computer Society Conference on Computer Vision and Pattern Recognition*. San Francisco, CA, USA: IEEE, 2010, pp. 2544–2550, doi: 10.1109/CVPR.2010.5539960.

[16] J. F. Henriques, R. Caseiro, P. Martins, and J. Batista, “Exploiting the circulant structure of tracking-by-detection with kernels,” in *Computer Vision – ECCV 2012*, ser. Lecture Notes in Computer Science, A. Fitzgibbon, S. Lazebnik, P. Perona, Y. Sato, and C. Schmid, Eds., vol. 7575. Berlin, Heidelberg: Springer, 2012, pp. 702–715, doi: 10.1007/978-3-642-33765-9_50.

[17] H. Grabner, M. Grabner, and H. Bischof, “Real-time tracking via online boosting,” in *Procedings of the British Machine Vision Conference 2006*, M. Chantler, B. Fisher, and M. Trucco, Eds. British Machine Vision Association, 2006, pp. 6.1–6.10, doi: 10.5244/C.20.6.

[18] D. Held, S. Thrun, and S. Savarese, “Learning to track at 100 fps with deep regression networks,” *European Conference on Computer Vision (ECCV) 2016*, 2016, doi: 10.48550/ARXIV.1604.01802.

[19] Z. Kalal, K. Mikolajczyk, and J. Matas, “Forward-backward error: Automatic detection of tracking failures,” *2010 20th International Conference on Pattern Recognition*, pp. 2756–2759, 2010, doi: 10.1109/ICPR.2010.675.

[20] ——, “Tracking-learning-detection,” *IEEE Transactions on Pattern Analysis and Machine Intelligence*, vol. 34, no. 7, pp. 1409–1422, 2012, doi: 10.1109/TPAMI.2011.239.

[21] N. Dardagan, A. Brdanin, D. Džigal, and A. Akagic, “Multiple object trackers in opencv: A benchmark,” *2021 IEEE 30th International Symposium on Industrial Electronics (ISIE)*, pp. 1–6, 2021, doi: 10.1109/ISIE45552.2021.9576367.

[22] Blender Foundation. (2025) Blender. [Online]. Available: https://www.blender.org/download/releases/4-3/